Magnetic linear dichroism in spin-resolved Fe 2*p* photoemission

F. U. Hillebrecht, Ch. Roth, H. B. Rose, W. G. Park, and E. Kisker
Institut für Angewandte Physik, Heinrich-Heine Universität Düsseldorf, D-40225 Düsseldorf, Germany

N. A. Cherepkov*
Universität Bielefeld, Fakultät für Physik, P. O. Box 10 01 31, D-33501 Bielefeld, Germany
(Received 11 August 1995)

Linear magnetic dichroism is studied for the Fe 2*p* level by angle- and spin-resolved photoemission with high energy resolution. The dichroism occurs in angle-resolved experiments for a geometry as in the transverse magneto-optic Kerr effect, i.e., on reversal of sample magnetization in the direction normal to the plane defined by light polarization and electron emission. The large spin-orbit splitting allows us to investigate the $j=1/2$ and $j=3/2$ states separately. Spin analysis allows differentiation between polarization effects related to exchange and spin-orbit interactions. The results are discussed in the framework of an atomic model, where the exchange interaction between the magnetic *d* shell and the core hole lifts the degeneracy of magnetic sublevels of the core hole spectrum. The model is able to explain the general trend in the spectra, but does not fully account for the observed shapes of the $j=3/2$ peaks. The analysis shows that the dichroism is governed by the spin polarization parameter which determines the spin-orbit-induced spin polarization. This shows that if there is a magnetic dichroism then there is a finite spin-orbit-induced spin polarization. The rich structures observed in our complete experiment are evidence for the influence of many-electron effects in the Fe 2*p* spectrum. [S0163-1829(96)01718-3]

INTRODUCTION

The electronic structure of magnetic materials, which provides the key for understanding their properties in general, and the basis of their magnetic properties in particular, is being studied by numerous electron spectroscopic techniques. Spectroscopies involving explicitly those states which carry the magnetic moment, i.e., the *d* states of transition metals, or the *f* states of rare earths, are photoemission, x-ray absorption, and emission, etc. Apart from such techniques, core level spectroscopies which do not directly involve the magnetic states, e.g., x-ray photoemission, are useful since these spectra also are influenced by the interaction between the localized core hole generated by photoemission and the magnetic valence states. The earliest example of a magnetic effect of this type in core level photoemission spectra is the occurrence of a satellite in the 3*s* photoemission spectrum of 3*d* transition-metal magnets, which is caused by the exchange interaction between the remaining, unpaired 3*s* electron and the 3*d* electrons.[1] Since this interaction is comparatively large, the associated difference in binding energy is several eV (4.5 eV for Fe), and can easily be measured. This splitting and intensity ratio have been used in numerous examples as an indicator for the presence and size of a magnetic moment.[2] For other core levels, the core-valence exchange interaction is much smaller, so that the influence of exchange can only be studied by spin-resolved photoemission. As an alternative to spin-resolved photoemission, one may make use of magnetic dichroism in photoemission: core level spectra show under certain conditions changes of line shapes and/or intensity upon change of the relative orientation of the light polarization and magnetization.[2–5]

To date, the largest number of experiments of this type has been performed in x-ray absorption using circularly polarized radiation.[2–4] In such an experiment the core electron is excited to an unoccupied state near the Fermi level E_F. Circular dichroism in x-ray absorption can be understood as resulting from a spin-dependent excitation of core electrons into spin-polarized final states immediately above the Fermi level.[2] The spin dependence comes about due to the coupling of the angular momentum of the photon to the total angular momentum of the electron, which is reflected in the dipole selection rule $\Delta m_j=\pm 1$ for σ^+ or σ^- light, respectively. Since the spin and orbital angular momenta of the electron are coupled by spin-orbit interaction, the spin polarization of photoelectrons is coupled to photon helicity. Spin and orbital moments of the incompletely filled valence shell can be probed by comparing excitation cross sections for different relative orientations of light helicity and sample magnetization.[6,7]

When comparing photoabsorption to photoemission, there are two important differences. The first difference is that in a photoemission experiment, the photoelectron is excited to a state far above the Fermi level, where one can usually neglect exchange and spin-orbit interactions.[5] In other words, the continuum final states available for the photoelectron are of equal density for both kinds of spin; there is no spin polarization in this continuum of empty states. Secondly, it is close to impossible to perform a truly angle-integrated photoemission experiment on solids, so any experiment has a finite angular acceptance. Consequently, the angular dependence of the excitation cross section has to be taken into account, whereas in photoabsorption one measures the angle-integrated excitation cross section. To stress the angle-resolving nature of photoemission experiments, one may characterize the effects discussed here as magnetic dichroism in the angular distribution (MDAD).

In general, magnetic dichroism is associated with the combined influence of spin-orbit and exchange interactions. It is known from experiment that both effects by themselves are large enough to cause significant spin polarization in core level spectra; the influence of exchange interaction is known from spin-resolved photoemission on core levels which began a couple of years ago with experiments on the Fe $3p$ level.[8] Since then, the $3s$ (Refs. 9 and 10) and $3p$ (Refs. 11 and 12) core levels of the $3d$ ferromagnets have been studied using synchrotron radiation. Studies of the Fe $2p$ core levels have been performed recently using unpolarized Mg $K\alpha$ radiation, where 1.6 eV total energy resolution was reached.[13] Spin-orbit-induced spin polarization[14] has been known for a long time from experiments on noble gases, adsorbates, etc.[15] This phenomenon is expected for any subshell with nonzero orbital angular momentum l provided the spin-orbit splitting is resolved. Recently, this polarization has been observed for Cu $3p$ and $2p$ (Ref. 16) and W $4f$ (Ref. 17) emission excited by linearly polarized light. For circularly polarized light the spin polarization may have finite components in all three directions in space[15] while for linear polarized light the electron polarization is normal to the plane defined by the light polarization (the electric field vector of the light) and the direction of electron emission.[14] In the latter case, the polarization is caused by an interference between the different continuum final states accessible for the photoelectron from an initial core state with angular momentum $l>0$. In a naive picture, magnetic dichroism occurs if the spin polarization due to spin-orbit interaction is collinear with the axis of magnetization. This is consistent with the reports on magnetic circular dichroism (MCD) in non-spin-resolved photoemission by Baumgarten *et al.*[5] and Schneider *et al.*[18] for bcc Fe, by Pappas *et al.*[19] for fcc Fe on Cu, and by van der Laan *et al.*[20] for Ni $3p$. Also, the observation of circular dichroism for helicity and magnetization perpendicular to each other[18] with the electron emission in the plane spanned by these two directions is consistent with this picture.

In this publication we report on magnetic dichroism in Fe $2p$ photoemission excited by linearly polarized light. This dichroism occurs in angle-resolved experiments for a geometry as in the transverse magneto-optic Kerr effect, i.e., on reversal of sample magnetization in the direction normal to the plane defined by light polarization and electron emission.[21] The magnetization is parallel to the spin-orbit-induced spin polarization in nonmagnetic materials in this geometry. Linear magnetic dichroism for the Fe $3p$ level was recently reported by us,[21] and has been confirmed by a number of other groups,[22] also for other core and valence levels. As will be discussed below, the angular dependence of the dichroism is the same as that of the transverse magneto-optic Kerr effect. In the context of this publication, we only address linear dichroism in transverse geometry as described above, which has to be distinguished from the linear dichroism occurring for magnetization either parallel or perpendicular to the polarization.[21]

Analysis of the $3p$ level is complicated by the fact that exchange and spin-orbit interactions are of comparable size, such that the validity of LS coupling is questionable.[22] For the Fe $2p$ level, the spin-orbit interaction is much larger than that of the $3p$ level, leading to two well-separated final-state peaks for $j=\frac{3}{2}$ and $j=\frac{1}{2}$. Preliminary accounts of this work have been presented earlier.[23] In the present comprehensive report we include a discussion of the results in the framework of an atomic model.[24] The exchange interaction between magnetic d states and the core hole is important for magnetic materials. In the model used here, it is assumed that the effect of the exchange interaction is to lift the m_j degeneracy of the core hole state with $j=\frac{1}{2}$ or $\frac{3}{2}$, like the magnetic field in the Zeeman effect. No other structure due to the core-valence interaction is considered. The theory is discussed in more detail separately.[24,25] Here we apply this theory primarily for the qualitative discussion of the features observed in experiment. In principle, the type of magnetic dichroism considered here is expected to occur, and has in fact been observed with excitation by unpolarized radiation.[26,27,13]

Since magnetic linear dichroism comes about because of the combined influence of spin-orbit and exchange interactions, its basic properties can be derived from the effects generated by each of these interactions on its own. The early study of the spin-orbit-induced spin polarization in Ar and Xe photoemission spectroscopy (PES) showed a vanishing polarization in the angle-integrated intensity.[14] The experiments on Cu $3p$ and $2p$ (Ref. 16) show that there is a sufficiently large $l-1$ cross section for the levels and energy range of interest here. For the Fe (and Co) $3p$ level, the angular dependence has been studied, revealing the influence of photoelectron diffraction, and showing a vanishing dichroism in the angle-integrated signal,[28] in analogy with the disappearance of the integrated spin polarization for nonmagnetic materials. Kuch *et al.* confirmed the angular dependence expected from atomic theory in an experiment designed to avoid the influence of diffraction by the crystal lattice[29] by fixing the emission direction with respect to the crystal while varying the angle of light incidence.

A number of authors have presented theoretical models relevant to the experiment discussed in this work. Thole and van der Laan[30] analyzed the origin of spin polarization and dichroism in core level spectra in the context of an atomic model. Atomic means that the magnetic d states are characterized by their spin and total angular momentum, and as a consequence the spectra show strong multiplet features which are common for spectra of ionic compounds. The theory is highly successful for describing the $4f$ spectra of rare earths which are localized. Also, Ni circular dichroism could be well described by modeling the electronic structure of Ni as a linear combination of localized d^8, d^9, and d^{10} configurations.[20] Imada and Jo[31] performed calculations similar to the atomic model. An analysis of the dichroism in general terms with an emphasis on the angular dependence was presented by Venus *et al.*,[32,33] and also Thole and van der Laan refined their model with respect to angular resolution.[34] Venus *et al.* placed special emphasis on the possible influence the crystal symmetry may have on the magnetic dichroism. Sum rules,[6] which have proved so useful in x-ray absorption,[7] exist also for photoemission. However, for photoemission out of filled inner shells of transition metals, integration of, e.g., the dichroism spectrum over energy should yield zero, as also the moment in the filled core shell is zero. Recently, it was shown that analysis of the statistical moments of the spectra yields information on

ground-state properties.[35,36] Similar relationships were derived some time ago in the context of the 3*s* spectra of Fe and other 3*d* magnetic systems by Kakehashi.[37] The important feature of the statistical moment analysis is that it allows one to extract ground-state properties from photoemission spectra without the necessity to choose between a localized or delocalized description of the system. It is of interest to explore the potential of such an analysis, as this would presumably be free from variation of the matrix elements through the relevant part of the spectrum, which may be a source of uncertainty in the sum rules for x-ray absorption. Fully relativistic calculations using multiple-scattering formalisms[38] were performed by Ebert *et al.* for Fe 2*p* MCD,[39] and recently also for MLDAD,[40] and by Tamura *et al.*[41] for Fe 3*p*. This approach has the advantage that it does not contain any adjustable parameters or input from experiment, and promises to provide a detailed account of the variation of the magnetic dichroism with emission direction which is caused by scattering from the solid state environment. The close relationship between the type of linear dichroism studied here and circular dichroism became apparent from experimental[42] as well as from theoretical work.[31,33,35,56]

EXPERIMENT

The experiments were performed at the new undulator beamline[43] BW3 at HASYLAB, Hamburg, shortly after the Doris ring became a dedicated synchrotron radiation source. Synchrotron radiation is generated by a device equipped with three different magnet structures to cover the range from 15 to 1800 eV with the first harmonic. To allow for quick changeover from one to another magnet structure during operation of the storage ring, the magnet structures are mounted on two revolving supports. The monochromator is a modified SX700 plane-grating type, complemented by a toroidal refocusing mirror behind the exit slit.[43] The samples were thin films of Fe grown epitaxially on W(110) by electron beam evaporation, following the procedures described by Gradmann *et al.*[44,45] The evaporation rate was about 0.5 Å/s. During growth of the first monolayer the substrate was heated to about 100 °C.[44] The thickness of the Fe film was chosen larger than 70 Å, so that the easy axis for magnetization was along the in-plane (100) direction of the W(110) surface. The low-energy electron diffraction (LEED) patterns of the W(110) substrate and the Fe film were of similarly high quality. The experimental geometry is sketched in the inset in the top panel of Fig. 1. Due to the thin-film nature of the magnetic sample, the magnetic state can be assumed to be single domain after applying field pulses of 80 Oe. All data were taken in remanence. The light was incident under 15° measured to the surface, along the (110) direction of the W surface. In previous experiments performed at BESSY,[21] there was an angle of 5° between the direction of light incidence and the (110) direction of the substrate. Since this angle was very small, the geometries can be regarded as identical. This is also demonstrated be Fe 3*p* spectra taken in the present geometry at 90 eV photon energy being identical to the ones reported earlier.[21] Photoelectrons were collected in normal emission with a geometrical angular acceptance of the spectrometer entrance lens of about 8° full cone. However, due to the retardation of the photoelectrons from about 100 eV kinetic energy to the pass energy (10 eV) of the spectrometer, the effective angular acceptance was smaller, and depends on the kinetic energy. Around 100 eV kinetic energy we estimate an angular acceptance of the order of 2° full cone for 10 eV pass energy. The total energy resolution, including the finite energy spread of the photons, was about 0.7 eV.

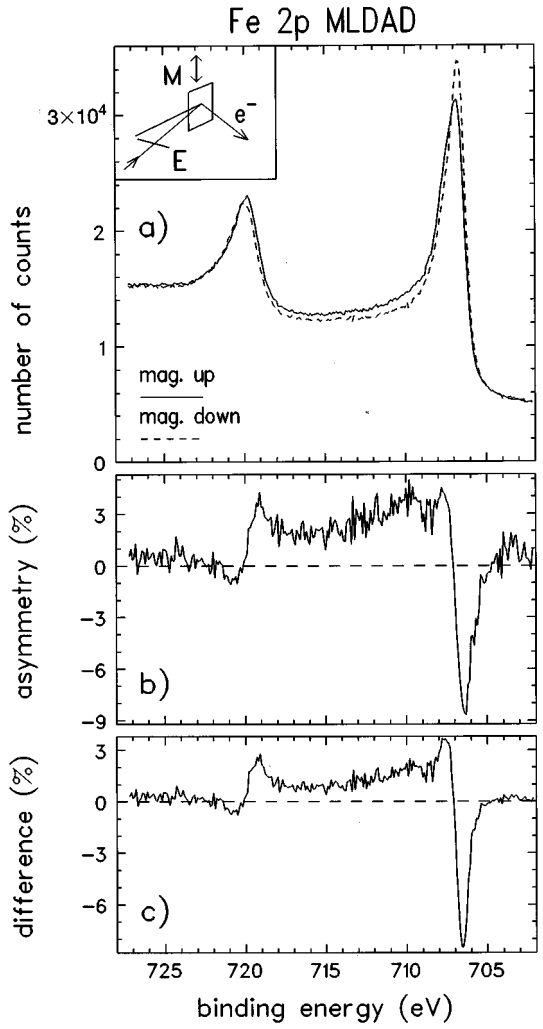

FIG. 1. (a) Fe 2*p* photoemission spectra taken with 879 eV linearly polarized photons for magnetization up (full line) and down (dashed). Inset shows the experimental geometry: linearly *p*-polarized radiation is incident under 15° (measured to the surface), electrons are collected in normal emission. (b) Asymmetry. (c) Normalized intensity difference (see text).

The spin polarization of the photoelectrons was analyzed by very-low-energy (VLEED) scattering off a magnetized Fe(100) surface.[46,9] In spin-resolved electron spectroscopy an apparent spin polarization may occur due to apparatus asymmetries. In experiments on magnetic materials, these can be excluded by reversing the sample magnetization. However, in measurements under excitation conditions leading to magnetic dichroism the spectra obtained for opposite sample magnetizations are no longer equivalent, so that the apparatus asymmetry cannot be removed by averaging data taken with opposite sample magnetizations. For our spin de-

tector one may take data with a scattering energy for which there is no spin dependence; remaining intensity differences should then reflect the apparatus asymmetry. Alternatively, one may analyze the spin polarization for spectral regions (away from the main peaks) where the dichroism should vanish, so that the spin polarization should not depend on sample magnetization. This should, for example, be the case on the low-binding-energy (BE) side of the Fe $2p_{3/2}$ photoemission peak, since the photoemission peaks of the $3p$ shell are far away in energy, and the total intensities are usually the same for both sample magnetizations. Consequently, the apparatus asymmetry can be fixed by requiring the spin polarizations on the low-BE side of the Fe $2p_{3/2}$ peak to be the same for both sample magnetizations. The two procedures yield consistent results. For the measurements considered in this publication the apparatus asymmetry was smaller than 1%.

For experiments depending on the light polarization, it is important to address the possibility of a change of light polarization by the material under investigation. Lately, a number of reports have appeared on Faraday rotation in the soft-x-ray regime by ferromagnetic Fe.[47] However, in all those experiments the rotation is only appreciable for photon energies close to core level thresholds. Since in photoemission one uses photon energies well above the binding energy of the level to be investigated, the polarization state of the light will not be affected. Such effects will, however, be a serious problem in resonant photoemission, where one measures photoemission from a shallow core level, tuning the photon energy to the binding energy of a deeper core level.

SPIN-INTEGRATED LINEAR DICHROISM

Figure 1 shows spin-integrated Fe $2p$ spectra taken with photons of 879 eV for a magnetized Fe film. The spectrum shows the $j=\frac{3}{2}$ and $j=\frac{1}{2}$ final states, separated by 13 eV due to spin-orbit interaction. The spectrum averaged over both sample magnetizations agrees with earlier reports, as do the binding energies for the two final states. The magnetization direction was normal to the reaction plane, as indicated in the inset in Fig. 1. Comparing the spectra for the two magnetization directions, one finds that they change when the sample magnetization is reversed: For magnetization up the $j=\frac{3}{2}$ peak intensity is reduced, and the peak has slightly higher binding energy than for magnetization down. For the $j=\frac{1}{2}$ final state, the situation is reversed: for magnetization up the $\frac{1}{2}$ peak is *higher* and at *lower* binding energy than for magnetization down. This difference in line shape and/or intensity is the magnetic linear dichroism discussed here.

A common representation of the changes associated with the magnetic dichroism is the asymmetry, which is the difference of the spectra for the magnetization up and down, divided by the sum. Figure 1(b) shows this asymmetry. Starting at low binding energy, the $\frac{3}{2}$ state first shows a negative asymmetry, changing to positive, while for the $j=\frac{1}{2}$ state the asymmetry is positive at low binding energy, and changes to negative. Apart from that, the asymmetry does not go to zero between the two peaks. This is also apparent in the original spectra in Fig. 1(a). In principle, this behavior may be caused by the background of secondary electrons, which is generally associated with photoemission from solids, and whose intensity should be proportional to the primary intensity. However, the intensities in primary peaks are very similar to each other, since the increased width of the peak for magnetization up compensates the higher peak intensity of the line for magnetization down. Consequently, the finite dichroism in the region between the two peaks cannot be due to secondaries. A finite asymmetry between the $\frac{3}{2}$ and $\frac{1}{2}$ lines has also been found in circular dichroism for the Fe $2p$ level.[5,18,19]

In order to reduce the influence of the secondary background on the quantitative dichroism result, one may consider the *difference* between the spectra for the two magnetizations, rather than the asymmetry. To allow a quantitative comparison, the spectra for the two magnetizations were added, and the intensity on the high-binding-energy side of the Fe $2p_{3/2}$ line was subtracted as a constant background. The difference spectrum was then normalized to the *peak* intensity of this spectrum. The difference spectrum obtained in this way is shown in the lowest panel of Fig. 1. It is similar to the asymmetry spectrum; however, for obvious reasons the scatter of the data in regions of low intensity is reduced.

Qualitatively, the observed linear dichroism has a similar appearance to the circular dichroism for bcc Fe,[18] and for fcc Fe on Cu.[19] A detailed comparison is, however, difficult due to the improved energy resolution in the present experiment. By applying a suitable broadening to our data, one finds that the dichroic asymmetry decreases by a factor of 2–3 when the resolution changes from 0.7 to 3 eV. This indicates that the linear magnetic dichroism is of the same order of magnitude as the circular dichroism observed for fcc or bcc Fe.[18,19] For the Fe $3p$ level it was shown that the line shapes of the circular and linear dichroisms are virtually identical.[42]

Figure 2 shows a detailed view of the dichroism in the neighborhood of the Fe $2p_{3/2}$ photoemission peak for three different photon energies for a different sample. The maximum of the difference occurs at 706.5 eV, at slightly smaller binding energy than the photoemission peak (706.8 eV). In all cases, the positive lobe is weaker than the negative one. Although the data cover only a limited photon energy range, they show a decrease of the dichroism from 10% for energies within 100 eV of threshold to about 7% at 879 eV. An interesting feature can be seen in this graph, namely, that the dichroism shows a structure 2–3 eV away from the main photoemission peak, although there is no strong feature in the original data at this energy. This feature is reproducible, and was found in all spectra; it is also recognizable in Fig. 1.

Since the original spectra do not show a clearly recognizable structure at this energy, one may attribute this feature to different line shapes of the lines for the two magnetization directions. Core level photoemission line shapes of metallic solids are affected by excitation of electron-hole pairs in the vicinity of the Fermi level.[48] The number of such excitations depends on — among other things — the combined density of states around the Fermi level. In a ferromagnetic solid, the densities of states for majority and minority spins at the Fermi level are different. From our spin-resolved measurements to be shown below we also know that the spin polarization of the Fe $2p$ photoemission peak changes when the magnetization is reversed. If also the cross section for excitation is spin dependent, the line shapes of majority- and minority-spin portions of a photoemission peak will be dif-

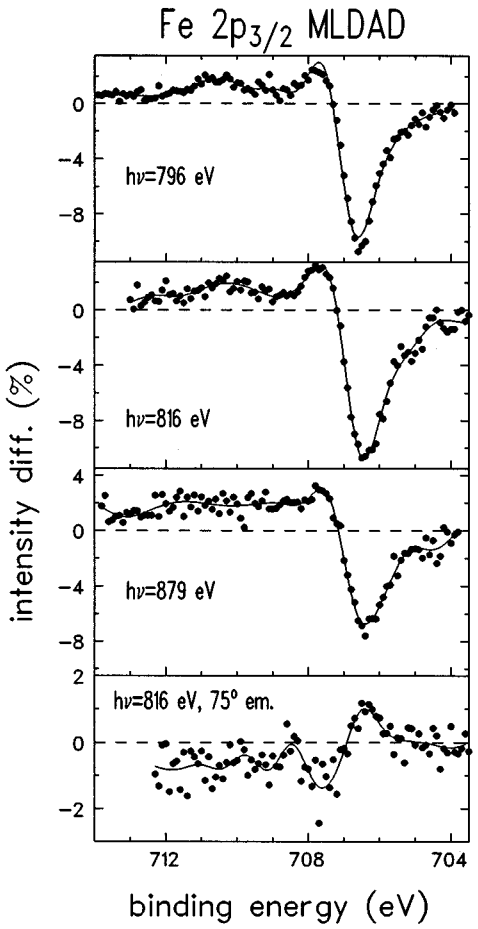

FIG. 2. Detail of the magnetic linear dichroism at the Fe $2p_{3/2}$ level for 796, 816, and 879 eV photon energy (top to bottom). Lowest panel shows dichroism for normal light incidence, and electron emission at 75° to surface normal.

ferent. For Doniach-Sunjic-type[48] line shapes this would result in different asymmetry indices. Also, the lifetime widths of majority and minority core holes may be different. These circumstances together may affect the line shapes such that the extra feature in the magnetic dichroism is generated.

Since the linear dichroism as studied here is similar to the circular one, it is meaningful to compare to the circular dichroism spectrum calculated by Thole and van der Laan.[30] They find, in fact, a feature reminiscent of the one observed here; however, there is much more structure beyond, also in the isotropic spectrum. These structures are essentially due to the localized nature of the *d* electrons in those model calculations, which led to discrete satellites. Consequently, the possibility of satellite-related features showing up in the dichroism cannot be completely excluded.

Finally we show in Fig. 2 how the dichroism is affected when the angle of electron emission is changed while the angle between light polarization and electron emission remains constant. In an atomic picture, i.e., neglecting solid state effects, the dichroism is determined solely by this angle, and a change of the dichroism can be caused, e.g., by photoelectron diffraction. The result is quite surprising. Not only does one find for emission at 15° to the surface a significant reduction of the dichroism, but even a *reversal* of sign compared to normal emission. Intuitively, one might expect a larger dichroism since spin-polarized LEED (SPLEED) experiments have shown that at room temperature the magnetic moment at the (110) surface of Fe is 30% enhanced over the bulk moment.[45] Clearly, the change of dichroism does not reflect — or at least not primarily — a change of the magnetic moment at the surface, but demonstrates the influence of photoelectron diffraction. This effect has to be taken into account for any detailed quantitative comparison between theory and experiment when the emission angle is varied. We note that the line shapes of the Fe $2p$ lines averaged over both magnetizations are virtually identical for both angles. A recent detailed study of the influence of photoelectron diffraction on the magnetic linear dichroism[28,49] has shown that large effects are quite common, but in agreement with the present observation no strong effect was observed in the spectral shape averaged over both magnetizations.

The angular dependence of the magnetic circular dichroism in Fe $2p$ photoemission was studied by Venus *et al.*[32] They also find quite dramatic changes of the dichroism with geometry; however, their data do not show a sign change. The results are analyzed by expanding the photoelectron wave into spherical harmonics, chosen such as to reflect the crystalline symmetry. For emission along high-symmetry directions, e.g., normal emission in our experiment containing two mirror planes, only some of the expansion coefficients are finite, so that at least the spectral dependence of the dichroism is not affected by the solid state environment. This means that sum rules should also be transferable from angle-integrated theory to an angle-resolving experiment. In contrast, for the emission in low-symmetry directions, i.e., the (non-normal) 75° emission in our case, all final-state waves allowed by dipole selection rules may contribute. In our 75° data, we note, however, that for the spin-integrated dichroism the deviation from the sum rule stating that the total intensities should be the same for both magnetizations is small. Furthermore, in this picture[32] no diffraction effects are included. For the Fe $3p$ and Co $3p$ levels it is known that photoelectron diffraction does affect the dichroism strongly, and may even lead to a sign reversal.[28,49]

SPIN-RESOLVED MAGNETIC DICHROISM

Before discussing the spin-resolved data, some remarks on spin-resolved core level photoemission data of ferromagnetic solids are in place. In spin-resolved photoemission spectroscopy of solids one usually finds that the background of secondary electrons is spin polarized. Since the secondary electrons are generated by higher-kinetic-energy features in the spectrum undergoing scattering processes, the spin polarization in the background results from a spin dependence of these scattering processes or from spin polarization in the primary features. The spin polarization in the primary features is first of all due to what in photoelectron diffraction is called the source function, i.e., with which polarization the photoelectrons emerge from the site from which they are being released. In a three-step model, this polarization may be modified as the photoelectrons traverse to and through the surface. The primary spin polarization may be affected by elastic as well as inelastic spin-dependent scattering. Spin-dependent inelastic scattering obviously will result in reduc-

ing the elastic intensity of one spin channel more than the other, thereby affecting the spin polarization measured in the primary photoemission peak. Since in elastic scattering the energy is unchanged, the spin polarization can only be affected due to the angular dependence of the elastic scattering. If, e.g., the source function is angle dependent, i.e., anisotropic, and the elastic scattering is isotropic, then the observed spin polarization depends on the direction of observation. The spin dependence of the mean free path can be inferred, e.g., from an experiment where one measures the spin polarization of an emission feature of a nonmagnetic material which is covered by a magnetic material. If such a feature acquires a spin polarization, one can conclude that this is due to a spin-dependent scattering cross section. Such experiments have been reported by Pappas *et al.*[50] For low kinetic energies they find a spin-dependent mean free path, while at 50 eV the spin dependence disappears. In our experiments the kinetic energy of the photoelectrons is between 80 and 200 eV, where spin dependence of the mean free path is small.

In our view the best empirical evidence for the influence of scattering on the spin polarization measured for a photoemission feature derives from measuring the change in polarization which is acquired by an electron beam — polarized or unpolarized — when it is scattered off a magnetic surface. If we consider elastic scattering from a single-crystal surface, this experiment is a spin-polarized LEED experiment. Such spin-polarized LEED experiments have been reported by Waller and Gradmann for Fe(110) grown on W(110), as is used also in this work, for 30–120 eV incident energy and 10°–45° incident angles.[44] For energies around 100 eV, it is found that the exchange asymmetry is in most cases positive, between $+2\%$ and $+5\%$. Therefore the exchange asymmetry is *opposite* to the minority polarization commonly observed in core spectra shown below. Spin-orbit asymmetries are found to be much smaller. In the context of our experiment they can contribute only to the spin-orbit polarization. Hopster, Raue, and Clauberg[51] performed an inelastic scattering experiment on an Fe-based metallic glass between 45 and 180 eV incident energy. In that work, there may be evidence for a small minority polarization in the elastic beam at low energy (45 eV); however, the polarization is negligible at 180 eV incident electron energy. This indicates that a minority-spin polarization as observed here, e.g., in Fig. 3, lower panel, is unlikely to be caused by spin-dependent scattering. Furthermore, one may derive from an elastic scattering experiment an estimate about what fraction of the intensity on the high-binding-energy side of a primary photoemission peak is due to secondary electrons. It is apparent from the data in the literature that only a small fraction of the steplike intensity increase underlying the Fe 2p peaks is caused by secondaries. This can be further substantiated by comparing the relative step heights for different core levels: If the step is exclusively caused by secondaries, the number of secondaries relative to the intensity in the primary peak should be the same for all photoemission peaks, provided one chooses the photon energies such that the primary peaks occur with similar kinetic energy. Inspecting, e.g., the Fe 3s spectrum measured with 250 eV photons,[9] we see that here the step in the secondary background from the low- to the high-binding-energy side of the peak is much smaller relative to the peak than for 2p levels. This indicates that a portion of the step associated with the 2p spectrum is caused by effects other than inelastic scattering. Consequently, the ratio of the step height relative to the primary intensity — in whichever way these are to be measured — cannot be used as a measure for the inelastic spin-dependent scattering cross sections. Only the background on the low-BE side of the $j=\frac{3}{2}$ state is a background of predominantly secondaries, since spectral features with higher energies — the L Auger lines and M photoemission lines — are sufficiently far away. The intensity on the high-binding-energy sides of the peaks must contain some other primary features, i.e., satellites, which are remnants of atomiclike multiplets.

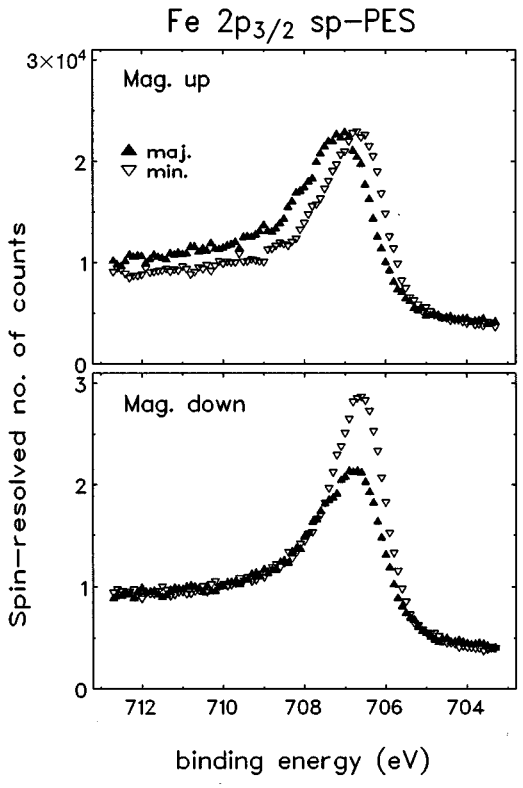

FIG. 3. Spin-resolved magnetic linear dichroism for Fe $2p_{3/2}$ photoemission ($h\nu=819$ eV).

Figure 3 shows spin-resolved data for the Fe $2p_{3/2}$ level. For each magnetization, the spectrum is split up into the majority and minority components. For the conditions of the present experiment, the secondary background (on the low-BE side) is unpolarized. For magnetization up, one finds on the high-BE side a majority polarization of about 10%; the individual line shapes are fairly similar to each other, and the total polarization is small, as the intensities in the two peaks are essentially identical. The main difference between the spin-resolved spectra is a shift in binding energy of 0.8 eV. For magnetization down, there is a pronounced line-shape difference between the minority- and majority-spin spectra, and also an intensity difference (overall polarization about -17%). As argued above, a finite minority-spin polarization, which is stronger for the magnetization-down case, is not caused by spin-dependent (elastic or inelastic) scattering. An important feature present in the data for both

magnetizations is that the minority-spin component occurs with lower binding energy than the majority component. Intuitively, one would expect a behavior in line with Hund's rule, i.e., a lower excitation energy when the spin of the remaining core shell is parallel to the spin of the d electrons. In that case the ejected photoelectron has its spin antiparallel to the majority-spin direction, as is found here experimentally for the low-BE side of the Fe $2p$ peaks. The spin-resolved spectra for the two magnetizations indicate that line shapes and overall spin polarization are affected by reversing the magnetization.

These spectra are influenced by spin-orbit as well as by exchange interaction. Both interactions by themselves produce a spin polarization in the spectrum. In electron scattering it has been shown that it is possible to separate the polarization effects by adding the polarized spectra in different ways.[52] For core level photoemission excited by circularly polarized light an analogous procedure was suggested.[30,42] If majority is added to majority, and minority to minority, then the effect of reversing the magnetization is canceled. Observation of the dichroism requires reversing the magnetization; therefore this averaging removes the magnetic dichroism, and one is left with a spectrum representing the spin polarization induced by the exchange interaction between the core hole and the d electrons. This is shown in the upper panel of Fig. 4. As was noted above for the individual spin-resolved spectra, the minority emission occurs at lower binding energy in both cases, and this is also seen in the summed spectrum. Apart from the BE difference, the minority spectrum also has higher peak intensity and a narrower line shape than the majority component. A similar behavior has been observed for the Fe $3p$ spectrum if taken under conditions where no magnetic dichroism occurs.[8,11] The differences in BE and width cause a sign change of the exchange-induced spin polarization from minority on the low-BE side of the peak to majority on the high-BE side. For circularly polarized light, the difference between these two spectra has been termed the spin spectrum (denoted by I^{01}) in Ref. 30, and is also shown in Fig. 4.

By adding the spectra for a fixed direction of spin in the laboratory frame of reference, independent of magnetization, the exchange-induced polarization is removed, as majority for one magnetization is added to minority for the other. Consequently, if the spectra so obtained are different from each other, then there is a spin polarization which is caused by spin-orbit interaction. This is shown in the lower panel of Fig. 4. The line shapes and intensities of the two different spin channels are more similar to each other than in the exchange case. The most important difference to the exchange polarization is that the sign of the spin-orbit polarization does not change through the spectrum. The spin-orbit-induced polarization is determined by coupling between spin and orbital momenta. For a spin-orbit splitting of 13 eV, as for Fe $2p$, the admixture of $j=\frac{1}{2}$ states to the $j=\frac{3}{2}$ final state is small, so that indeed the spin-orbit-induced polarization should not change its sign within one of the substate spectra.[30]

Figure 5 shows the equivalent sum spectra for the Fe $2p_{1/2}$ level. As for the $j=\frac{3}{2}$ level, exchange shifts the minority peak by 0.5 eV to lower binding energy compared to the majority. The peak intensities as well as the line shapes are

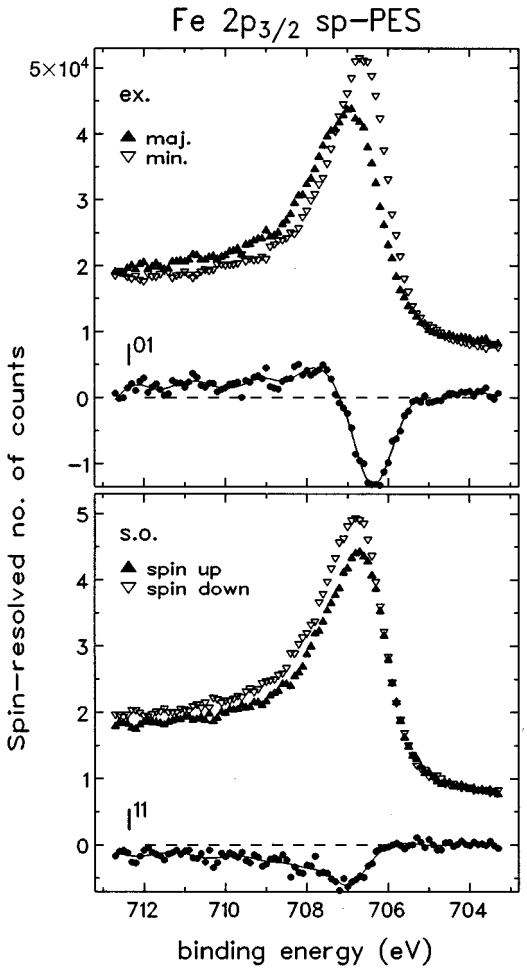

FIG. 4. Spin-resolved Fe $2p_{3/2}$ photoemission spectra, representing exchange- (top) and spin-orbit-induced (bottom) spin polarizations.

similar to each other. Both spectra show a shoulder on the high-BE side, which may be caused by residuals of atomic multiplet structure. In the secondary background, the majority polarization is larger on the high-BE side of the peak than on the low-BE side. The spectra for fixed spin direction in the laboratory frame of reference, which reflect the spin-orbit-induced polarization, are shown in Fig. 5(b). They appear with the same peak height and binding energy. The binding energies should be the same, since we have averaged over magnetization. Nevertheless, there is an overall polarization, since the base level of the up-spin peak is lower than that of the down-spin peak. This polarization is opposite to that found in the $j=\frac{3}{2}$ line.

DISCUSSION

For a qualitative description of the observed phenomena, we use an atomic model which is comprehensively covered in separate publications.[24,25] In this model the solid state effects are taken into account only by introducing the energy splitting of the magnetic sublevels of the core hole state. This energy splitting appears due to exchange interaction between the core and valence electrons, and is of the order of 1 eV for the $2p$ and $3p$ levels of Fe.[38–41] Therefore the hole state generated by photoemission will be characterized in the fol-

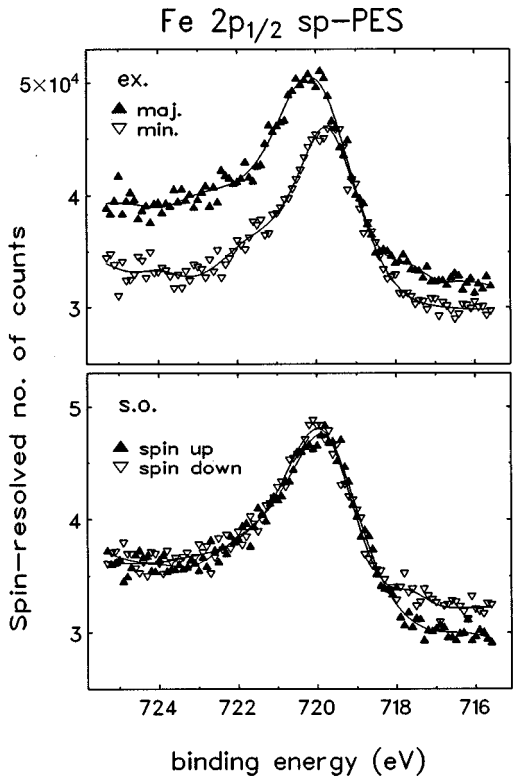

FIG. 5. Spin-resolved Fe $2p_{1/2}$ photoemission spectra, representing exchange- (top) and spin-orbit-induced (bottom) spin polarizations.

lowing by the quantum numbers $nljm_j$, where n is the principal quantum number, l is the orbital angular momentum and $j=l\pm\frac{1}{2}$ and m_j are the total angular momentum and its projection on the direction of sample magnetization. The effects of spin-orbit interaction in the continuum are neglected, as they are expected to be smaller than other solid state perturbations neglected in our model.

We first consider the spin-integrated magnetic dichroism in the angular distribution. For linearly polarized light and magnetization reversal perpendicular to the plane of incidence we obtain[24,25]

$$I_j^{\mathrm{MLDAD}}=\frac{\sigma_{nlj}(\omega)}{2\pi}\rho_{10}^n\sin 2\theta\begin{cases}2\sqrt{5}\,\eta^{3/2}, & j=\frac{3}{2}\\ -\sqrt{2}\,\eta^{1/2}, & j=\frac{1}{2},\end{cases}\qquad(1)$$

with

$$\eta^{1/2}=-2\,\eta^{3/2}=-\frac{3}{\sqrt{2}}[d_s d_d\sin(\delta_d-\delta_s)]/(d_s^2+d_d^2).\qquad(2)$$

For circular light polarization and magnetization reversal in the plane of incidence we obtain

$$I_j^{\mathrm{MCDAD}}=\frac{\sigma_{nlj}(\omega)}{2\pi}\rho_{10}^n\cos\theta\begin{cases}2\sqrt{5}(A^{3/2}+\frac{1}{2}\gamma^{3/2}), & j=\frac{3}{2}\\ -\sqrt{2}(A^{1/2}+\frac{1}{2}\gamma^{1/2}), & j=\frac{1}{2},\end{cases}\qquad(3)$$

where θ is the angle between the light beam and the surface normal, ρ_{10}^n are state multipoles[53–55] characterizing polarization of each magnetic sublevel, and A, γ, and η are a set of standard parameters used to characterize the spin polarization of photoelectrons ejected from unpolarized atoms,[56]

$$(A^{1/2}+\gamma^{1/2})=-2(A^{3/2}+\gamma^{3/2})=\left[d_s^2-d_d^2+\frac{1}{\sqrt{2}}d_s d_d\cos(\delta_d-\delta_s)\right]\Big/(d_s^2+d_d^2).\qquad(4)$$

δ_s and δ_d and d_s and d_d are phase shifts and reduced dipole matrix elements for the $p\rightarrow s$ and $p\rightarrow d$ transitions, respectively.[56]

The expression (2) shows that the linear dichroism is an interference effect governed by the spin polarization parameter η, and is only finite if there is a finite cross section for both $l+1$ and $l-1$ final states. For the circular case, the dichroism is present in the incoherent cross section. Furthermore, both the $l+1$ and the $l-1$ channels give mutually opposite contributions to the circular dichroism. This, and the contribution of an interference term, render a quantitative analysis much more difficult than in the linear case. Circular dichroism is small if $|d_d|\cong|d_s|$. This is, in contrast, the condition under which the linear dichroism is maximum. In the linear case, disappearance of dichroism can be caused either by one of the matrix elements going through zero, or by the phase shift difference going through a multiple of π. In the particular case of the $2p$ subshell, both matrix elements d_s and d_d do not have zeros,[57] and $|d_d|\gg|d_s|$. Consequently, MCDAD does not have zeros, while MLDAD will have zeros at photon energies where the phase shift difference goes through a multiple of π. So, in spite of the similarities between the observed linear and circular dichroism curves discussed above, these two cases have also essential differences, which can be exploited by comparing their photon energy dependences.

The fact that the core hole state is split into sublevels with a given projection of the total angular momentum m_j is conveniently described by state multipoles as described earlier.[24] Using the numerical values of state multipoles from Table I of Ref. 24, the relation (2) between $\eta^{3/2}$ and $\eta^{1/2}$, and the fact that the cross section σ_{nlj} for the $j=\frac{3}{2}$ state is two times larger than for $j=\frac{1}{2}$, one finds from (1) that the area under the MLDAD curve in the $P_{3/2}$ level should be four times larger than in the $p_{1/2}$ level. This is approximately fulfilled in the experimental curve shown in Fig. 1(b). The fact that the dichroism starting from low binding energies is first positive and then negative in the $p_{3/2}$ level, and first negative and then positive in the $p_{1/2}$ level, evidences that there is an opposite ordering of magnetic sublevels in these two levels, as was shown already by Ebert *et al.*[38,39] Indeed, according to (1) and (3), both linear and circular dichroism are proportional to the first-state multipole ρ_{10}^n which for different magnetic sublevels has the same sign (see Table I of Ref. 24) as the projection m_j.

Next we consider spin-resolved spectra, applying the general equations from Refs. 24 and 25 to our particular situation. One finds that for the spin-resolved spectra the third-state multipole ρ_{30}^n also gives a contribution, while for the non-spin-resolved spectra ρ_{20}^n is the highest-state multipole

TABLE I. The ratios of intensities of different magnetic sublevels of np hole states in spin-resolved spectra to those in spin-unresolved spectra for the geometry of experiment shown in Fig. 1 and linearly polarized light. $\boldsymbol{n}$ is the direction of the sample magnetization, $\boldsymbol{e}$ is the light polarization vector, and $\boldsymbol{s}$ is direction of spin.

		$j=3/2$			$j=1/2$	
m_j	3/2	1/2	−1/2	−3/2	1/2	−1/2
$\boldsymbol{e}\perp\boldsymbol{n}$, $\boldsymbol{s}\parallel\boldsymbol{n}$	1	0	1	0	0	1
$\boldsymbol{e}\perp\boldsymbol{n}$, $\boldsymbol{s}\parallel(-\boldsymbol{n})$	0	1	0	1	1	0
$\boldsymbol{e}\parallel\boldsymbol{n}$, $\boldsymbol{s}\parallel\boldsymbol{n}$	0	1	0	0	1	0
$\boldsymbol{e}\parallel\boldsymbol{n}$, $\boldsymbol{s}\parallel(-\boldsymbol{n})$	0	0	1	0	0	1

for the $p_{3/2}$ subshell[25] provided spin-orbit interaction in the continuum states is neglected.[24] Therefore the spin-resolved spectra are a more stringent test for the theoretical model.

Turning to spin-resolved spectra one finds for the minority-spin intensities of the $j=\frac{3}{2}$ final state[24,25] summed over both magnetizations

$$I_{3/2}(M\uparrow,s\uparrow)+I_{3/2}(M\downarrow,s\downarrow)=\frac{\sigma_{3/2}(\omega)}{2\pi}\left(\rho_{00}^{n}+\frac{1}{2}\rho_{20}^{n}+\frac{2}{\sqrt{5}}\rho_{10}^{n}+\frac{3}{2\sqrt{5}}\rho_{30}^{n}\right)(1+\beta-\tfrac{3}{2}\beta\sin^2\theta) \tag{5a}$$

and for the sum of majority-spin intensities

$$I_{3/2}(M\uparrow,s\downarrow)+I_{3/2}(M\downarrow,s\uparrow)=\frac{\sigma_{3/2}(\omega)}{2\pi}\left(\rho_{00}^{n}+\frac{1}{2}\rho_{20}^{n}-\frac{2}{\sqrt{5}}\rho_{10}^{n}-\frac{3}{2\sqrt{5}}\rho_{30}^{n}\right)(1+\beta-\tfrac{3}{2}\beta\sin^2\theta). \tag{5b}$$

These expressions contain only the angular asymmetry parameter β, but not the spin polarization parameter η. This reflects the fact that in these spectra we have removed the spin polarization due to spin-orbit interaction by summation. To construct model spectra, one has to evaluate this expression for each m_j sublevel by inserting the state multipoles from Table I of Ref. 24, convolute with the appropriate line shape, and add the contributions of the different m_j sublevels shifted in energy by the exchange splitting. The contributions of different m_j sublevels are proportional to the expression in the first bracket. Using Table I of Ref. 24 one finds that the minority component (5a) is different from zero only for the $m_j=\frac{3}{2}$ and $-\frac{1}{2}$ magnetic sublevels, while the majority component (5b) is different from zero for $m_j=\frac{1}{2}$ and $-\frac{3}{2}$ sublevels, *independent* of the angle θ. Table I shows the intensities in the spin-resolved spectra relative to those in the non-spin-resolved spectra obtained in this way. The different contributing levels explain qualitatively the shift of one spectrum relative to the other observed in Fig. 4(a). The spin spectrum shown in Fig. 4(a) should correspond to the difference of (5b) and (5a), which is proportional to the factors $-\frac{3}{4}$, $\frac{1}{4}$, $-\frac{1}{4}$, and $\frac{3}{4}$ for the magnetic sublevels $m_j=\frac{3}{2}$, $\frac{1}{2}$, $-\frac{1}{2}$, and $-\frac{3}{2}$, respectively. Taking into account the experimental resolution and the intrinsic width of these levels, there is a qualitative agreement between theory and experiment as far as the sign change through the spectrum is concerned; however, the magnitudes of the positive and negative lobes and the line shapes are not in agreement.

For the spectra with a fixed spin direction in the laboratory frame of reference one obtains analogously

$$I_{3/2}(M\uparrow,s\uparrow)+I_{3/2}(M\downarrow,s\uparrow)=\frac{\sigma_{3/2}(\omega)}{2\pi}[(\rho_{00}^{n}+\tfrac{1}{2}\rho_{20}^{n})(1+\beta-\tfrac{3}{2}\beta\sin^2\theta)+(\rho_{00}^{n}+2\rho_{20}^{n})\eta^{3/2}\sin2\theta], \tag{6a}$$

$$I_{3/2}(M\uparrow,s\downarrow)+I_{3/2}(M\downarrow,s\downarrow)=\frac{\sigma_{3/2}(\omega)}{2\pi}[(\rho_{00}^{n}+\tfrac{1}{2}\rho_{20}^{n})(1+\beta-\tfrac{3}{2}\beta\sin^2\theta)-(\rho_{00}^{n}+2\rho_{20}^{n})\eta^{3/2}\sin2\theta], \tag{6b}$$

where η^j is the spin polarization parameter defined above. These spectra have a similar structure with nonzero contributions from all magnetic sublevels. The two spectra given by (6a) and (6b) differ only by the sign of the term proportional to $\eta^{3/2}$. The experimental spectra shown in Fig. 4(b) are also rather similar in shape, but differ in magnitude. Subtracting (6b) from (6a) yields the spin-orbit spectrum [Fig. 4(b)], in which the relative sublevel intensities are -3, 1, 1, and -3 from $m_j=\frac{3}{2}$, $\frac{1}{2}$, $-\frac{1}{2}$, and $-\frac{3}{2}$, respectively, so that overall the negative contribution should prevail over the positive one, which is observed in the experiment [see the lower part of Fig. 4(b)]. Since the difference between these two curves is proportional to the parameter $\eta^{3/2}$, it is in principle possible to derive $\eta^{3/2}$ from this experiment.

The analogous derivation[25] for the $np_{1/2}$ sublevel yields

$$I_{1/2}(M\uparrow,s\uparrow)+I_{1/2}(M\downarrow,s\downarrow)=\frac{\sigma_{1/2}(\omega)}{\sqrt{2}2\pi}(\rho_{00}^{n}-\rho_{10}^{n})(1+\beta-\tfrac{3}{2}\beta\sin^2\theta), \tag{7a}$$

$$I_{1/2}(M\uparrow,s\downarrow)+I_{1/2}(M\downarrow,s\uparrow)=\frac{\sigma_{1/2}(\omega)}{\sqrt{2}2\pi}(\rho_{00}^{n}+\rho_{10}^{n})(1+\beta-\tfrac{3}{2}\beta\sin^2\theta). \tag{7b}$$

These expressions give the minority- (7a) and majority- (7b) spin spectra of the $j=\frac{1}{2}$ subshell. Inserting the state multipoles from Table I of Ref. 24, one finds that only the $m_j=-\frac{1}{2}$ magnetic sublevel contributes to the minority-spin channel, and only the $m_j=\frac{1}{2}$ sublevel contributes to the majority-spin channel, while the intensities should be equal. Taking into account a difference in the backgrounds, one can see that the corresponding experimental spectra shown in Fig. 5(a) have just that behavior, that is, the peaks have the same shapes and intensities and are shifted in energy. This allows one to derive the positions of the $j=\frac{1}{2}$ magnetic sublevels with fairly high precision directly from the experimen-

tal data shown in Fig. 5(a). We obtain from our data a splitting of 0.5 eV between the $m_j=-\frac{1}{2}$ and $\frac{1}{2}$ sublevels of the $j=\frac{1}{2}$ final state.

For the sums with a fixed direction of spin in the laboratory frame one obtains

$$I_{1/2}(M\uparrow,s\uparrow)+I_{1/2}(M\downarrow,s\uparrow)=\frac{\sigma_{1/2}(\omega)}{\sqrt{2}2\pi}\rho_{00}^{n}(1+\beta\,-\tfrac{3}{2}\beta\,\sin^2\theta+\eta^{1/2}\sin 2\theta), \tag{8a}$$

$$I_{1/2}(M\uparrow,s\downarrow)+I_{1/2}(M\downarrow,s\downarrow)=\frac{\sigma_{1/2}(\omega)}{\sqrt{2}2\pi}\rho_{00}^{n}(1+\beta\,-\tfrac{3}{2}\beta\,\sin^2\theta-\eta^{1/2}\sin 2\theta). \tag{8b}$$

Here, both magnetic sublevels give equal contributions to each of these sums since they contain only the state multipole of zeroth order, so that the spectra should have a maximum in the middle between two magnetic sublevels. They differ only by the sign of a term proportional to $\eta^{1/2}$, which will result in a difference in magnitudes of two peaks. In agreement with these theoretical conclusions, the sums of experimental spectral with a fixed direction of spin in the laboratory frame shown in Fig. 5(b) are very similar, with the maximum just in the middle between the maxima in Fig. 5(a) which correspond to the $m_j=\frac{1}{2}$ and $-\frac{1}{2}$ magnetic sublevels.

Subtracting the spectra for fixed spin direction in the laboratory frame of reference (6a) and (6b) and (8a) and (8b) from each other, one is left with expressions proportional to η. For a nonmagnetic system, e.g., for the case of photoionization of unpolarized atoms, this parameter describes the spin polarization of photoelectrons ejected by linearly polarized light, which appears due to spin-orbit splitting of atomic levels.[14,15] Therefore, what we have characterized in the discussion above as spin-orbit-induced polarization is described by the term proportional to the parameter η, in analogy to the spin polarization induced by spin-orbit interaction for nonmagnetic systems like Cu.[16] On the other hand, the expressions for the majority and minority spectra (5a) and (5b) and (7a) and (7b) do not contain the spin polarization parameter η. In the present model, for any value of η, including $\eta=0$, the sum spectra for majority and minority would be unchanged. Consequently, the difference between the majority and minority spectra shows the exchange spin polarization. This justifies our characterization of the sum spectra obtained either in terms of majority/minority or with respect to fixed spin direction as reflecting exchange- and spin-orbit-induced spin polarization. One has to keep in mind, however, that also the spectral shape of the spin-orbit polarization is influenced by the magnetic ground state of the material investigated, since for a magnetic material the m_j sublevels are not degenerate, as they are, for example, in Cu. Hence the natural way to discuss the spin-orbit polarization in a quantitative manner is by considering its energy integral, relative to the energy integral of the sum spectrum. The quantitative result may be influenced by photoelectron diffraction.

Concerning the spin-orbit polarization, the experimental spectra in Fig. 5(b) have the same peak height; however, the background under the two spectra is different, so that the spin-up intensity is larger. Consequently, there is a finite polarization of about $+10\%$. Again, this is governed by the spin polarization parameter $\eta^{1/2}$, which is related to the radial matrix elements and associated phase shifts for s- and d-like final states. Taking into account that $\sigma_{1/2}\eta^{1/2}=-\sigma_{3/2}\eta^{3/2}$, and using the state multipoles from Table I of Ref. 24, one finds from Eqs. (6a), (6b), (8a), (8b) that the difference between the two curves in Fig. 4(b) for the $j=\frac{3}{2}$ level integrated over the peak width should have the same magnitude, but opposite sign compared to the difference between the corresponding curves of Fig. 5(b) for the $j=\frac{1}{2}$ level. We can summarize this as a sum rule by saying that the total emission out of the 2p subshell should be unpolarized. Considering only the spin-orbit polarization in the peak regions, the polarization in the $\frac{1}{2}$ region is only about $\frac{1}{3}$ of what it should be according to this sum rule, even though it is opposite to that in the $\frac{3}{2}$ peak. The spin-orbit polarization on the high-BE side of the $j=\frac{3}{2}$ level and on the low-BE side $j=\frac{1}{2}$ is finite, showing a finite spin-orbit polarization also in the region *between* these two peaks. This appears to be related to the finite magnetic dichroism in this energy region. The finite integrated spin-orbit polarization may be related to the deviation of the observed branching ratio between the $j=\frac{3}{2}$ and $\frac{1}{2}$ final states, $R=2.3\pm0.1$, from the statistical value of 2.

The essential conclusion from the foregoing analysis is that the spin polarization can be classified with respect to exchange or spin-orbit effects. The exchange polarization is of minority type at the low-energy threshold of the $j=\frac{3}{2}$ level, changing sign to majority type somewhere in the spectrum. The spin-orbit-induced polarization has a certain sign for a given fine-structure component. The linear dichroism is proportional to the same spin polarization parameter which governs the spin-orbit-related spin polarization in nonmagnetic systems. This illustrates the interplay between spin-orbit and exchange interactions for the occurrence of magnetic dichroism.

For a more detailed comparison between experiment and model, we restrict ourselves to the $j=\frac{3}{2}$ state since in the $j=\frac{1}{2}$ state there is a good qualitative agreement between theory and experiment. We start by considering the spin-integrated dichroic spectra which follow from the atomic model. As an approximation for the input parameters for the particular situation of our experiment, we used the matrix elements, phases, and atomic asymmetry parameter β of Goldberg, Fadley, and Kono[58] for Ni at 1000 eV photon energy. The spectral shape is not affected by the absolute magnitudes of these parameters; furthermore, they do not vary strongly with photon energy or between Fe and Ni. For the splitting between the m_j sublevels, we used 0.5 eV as derived from the $j=\frac{1}{2}$ spectrum. The relative sublevel intensities obtained in this way are 2.86, 0.95, 1.08, and 3.23 for magnetization up in order of decreasing m_j; for magnetization down the sequence of intensities is reversed. Each sublevel was represented by Doniach-Sunjic line shapes[48] with $\alpha=0.4$, a Lorentzian width $\Gamma_L=0.4$ eV,[59,60] and a Gaussian of 0.7 eV to account for the experimental resolution. Figure 6 shows spin-integrated intensities for magnetization up and

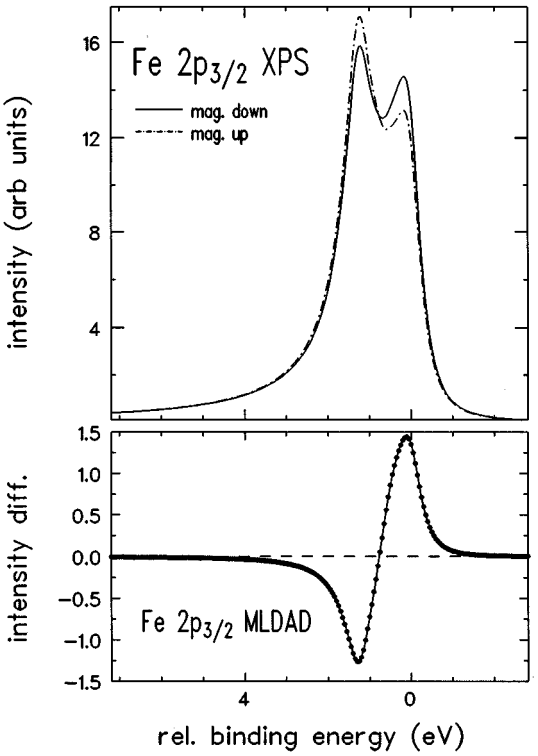

FIG. 6. Fe $2p_{3/2}$ spectrum derived from the atomic model using matrix elements and phases for Ni $2p$ at $h\nu = 1000$ eV from Goldberg, Fadley, and Kono (Ref. 58). The lines are composed of four Doniach-Sunjic lines with intensities as given in the text; the asymmetry index is $\alpha = 0.4$, the Lorentzian width is 0.4 eV, and the Gaussian broadening is 0.7 eV. Bottom panel shows linear magnetic dichroism.

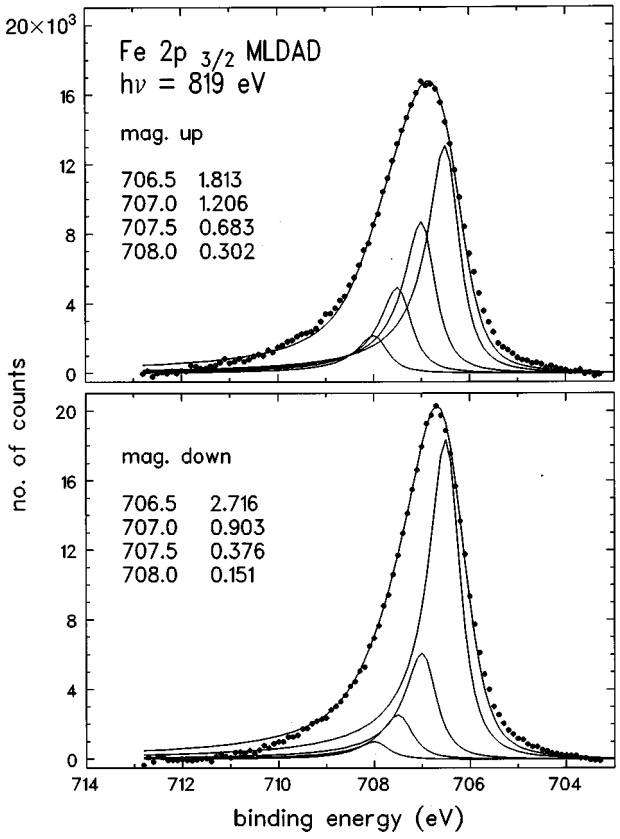

FIG. 7. Fit of the non-spin-resolved Fe $2p_{3/2}$ data after background subtraction by four equidistant Doniach-Sunjic lines. The numbers in the panels give the energies and intensities of the individual lines, chosen to give a sum close to 4. Dots show experimental data, lines show the four individual lines and their sum.

down obtained in this way, as well as their difference, i.e., the linear dichroism. The spectrum is dominated by the $m_j = \frac{3}{2}$ and $-\frac{3}{2}$ states, leading to the two peaks in the spectrum, whose intensities are affected by reversing the magnetization. The total intensities in the dichroic spectra are equal, in agreement with experiment. However, the line shapes are quite different from the experimental ones, the latter apparently having a significantly reduced intensity for the higher-binding-energy sublevels. If we maintain that the spectra are composed of four lines for the $j = \frac{3}{2}$ final states, then the experimentally observed line shape can only be explained if the individual lines have intensities quite different from those in atomic model. The cause for this deviation is not known at present.

A comparison of the spin-resolved model spectra with experiment would lead to a similar disparity as for the spin-integrated dichroic spectra. However, even though the model is not able to describe the spin-integrated dichroic spectra, it might yield an adequate description of the spin dependencies. As the present theoretical model does not give the correct intensities of the individual sublevels, we determine these intensities empirically from a fit to the spin-unresolved experimental data by four evenly spaced m_j sublevels. For that purpose experimental spectra free from secondary effects are desirable. Even though we argued above that the background is not entirely due to secondary electrons, we treated the experimental spectra as though this were the case. We used the standard procedure, assuming that the background at a given energy in the spectrum is proportional to the signal integrated up to that energy. Figure 7 shows the fits of experimental spectra with four Doniach-Sunjic lines[48] with asymmetry index $\alpha = 0.4$ and a Lorentzian lifetime broadening of 0.4 eV.[59] To account for the experimental resolution, the spectra were convoluted with a 0.7 eV Gaussian. We required the separation of the individual sublevels, which is caused by the exchange interaction, to be constant within the $j = \frac{3}{2}$ multiplet, and equal to 0.5 eV, since this is the exchange splitting found in the $j = \frac{1}{2}$ spectrum. Figure 7 shows the individual lines, as well as the combined spectra (full lines), compared to the experimental results (dots). The main features of the peaks can be well described by this procedure. There is some disagreement in the energy region at BE's higher than 710 eV; however, in this region the effect of possibly inadequate background subtraction, Lorentzian lifetime broadening, or many-body excitations may be significant.

For obtaining the spin-resolved spectra, we multiply the contribution of each magnetic sublevel in Fig. 7 by the appropriate factor given in Table I. The fact that only 0 and 1 occur in Table I reflects the theoretical result that the contributions of the individual sublevels should be fully polarized. The spectra obtained by this procedure are shown in Fig. 8. For comparison with experiment, we subtracted backgrounds in the same way as above. The general trend of the peak

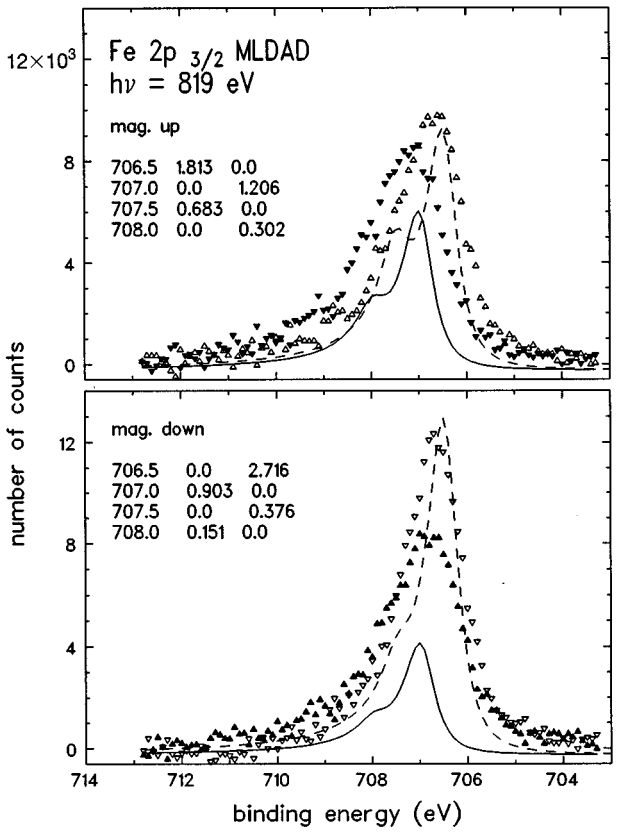

FIG. 8. Comparison of the spin-resolved Fe $2p_{3/2}$ data to spectra derived from the fit shown in Fig. 7. Filled triangles show majority-spin spectrum, empty triangles minority-spin spectrum. Lines give result of model spin polarizations combined with fit to measured spectra shown in Fig. 7; full and dashed correspond to majority and minority spin, respectively. The numbers in the three columns give energies and spin-up and spin-down intensities for each of the individual lines. Only two of the m_j sublevels contribute to each of the four spectra.

heights differing more strongly for magnetization down than up is correctly reproduced by the model. Also, the low-BE sides of the lines are generally steeper than the high-BE sides, which is due to the input intensities obtained as in Fig. 7. While these details are in agreement with experiment, the spin polarization derived in this way is always significantly larger and shows more structure than observed in experiment, despite the use of the empirical sublevel intensities. The experimental majority spectrum for magnetization down clearly has a lower threshold than in the model spectrum. While the atomic model describes the general trends in agreement with experiment, it appears that for the line shapes not only of the spin-integrated spectra, but also of the spin-resolved ones, some ingredient is missing in the description.

Within the atomic model the decrease of intensities of magnetic sublevels with negative m_j can be connected with the dependence of the initial-state wave function of m_j, but this effect hardly can account for the large differences which are apparent in Figs. 6 and 7. Another possibility is the influence of the term structure of the final state due to nonzero total angular momentum of the valence shell, which was also neglected in the atomic model. With regard to MLDAD asymmetry, it is clear[49] that photoelectron diffraction strongly influences the experimental result. This is impressively demonstrated by the reversal of sign of the dichroism observed with sample rotation, where the unchanged angle between light polarization and electron emission should yield the same dichroism (Fig. 2). The lower degrees of spin polarization which are obtained from experiment may be partly due to scattering processes, although it appears that the influence of spin-dependent scattering should be small. The 0.4–0.5 eV exchange splitting between the m_j sublevels which we derive from the $2p_{1/2}$ spectrum is significantly larger than the 0.27 eV calculated by Ebert,[38] but about a factor of 2 smaller than the value derived by Tamura *et al.*[41] for the 3p level. A different splitting would have a slight effect on the spin-resolved spectra derived from an analysis as shown in Figs. 7 and 8; however, no qualitative change is expected.

An aspect which is possibly relevant to our investigation is the suggestion of Tamura *et al.*[41] that, apart from spin polarizations generated exclusively by exchange or by spin-orbit interactions, there may be an interference between these two. If a geometry is chosen where these exchange and spin-orbit polarizations are normal to the direction of electron emission and orthogonal to each other, the interference generates a spin polarization in the third, longitudinal direction. In that situation there may still be a magnetic dichroism, since magnetization reversal reverses the exchange-induced polarization, and due to the interference with the fixed spin-orbit polarization a dichroism may occur. As yet there is no experimental evidence for this effect, and it is not clear how it may affect the magnetic dichroism and spin polarization in the experiment discussed here.

SUMMARY

We have investigated the magnetic linear dichroism in angle-resolved Fe 2p photoemission in transverse geometry, which is an *uneven* function of the magnetization, so that it appears on magnetization reversal. The dichroism is comparable in size to circular dichroism, despite the fact that it is an interference effect. Spin-resolved data have been obtained and analyzed with respect to spin-orbit- and exchange-induced effects. The distinction between these two mechanisms refers to the spin polarization being governed either by the spin-orbit interaction in the 2p level, making it independent of temperature, or by the exchange interaction. Spin-orbit-induced spin polarization does not depend on the sample being magnetically ordered. Using an atomic model, it was possible to interpret the main trends of the observed spectra, and to connect them with the parameters used to characterize the spin polarization of atomic photoelectrons. According to the atomic model, both linear dichroism and the spin-orbit-induced spin polarization are proportional to the spin polarization parameter η and go to zero if η goes to zero. Even though the observed line shapes were not in agreement with experiment, this result is general. The exchange-induced polarization, which depends on the splitting of the m_j levels, is not affected by the spin polarization parameter η. The exchange-induced spin polarization in pure form can be measured either in a geometry in which there is no magnetic dichroism, or by averaging over both magneti-

zations. From the analysis of the spin-resolved data for the p_{12} state we determined the splitting between the m_j sublevels to $0.5+0.1$ eV.

The rich structure observed in the spin-resolved spectra is at present not fully understood. The spin-orbit polarization apparently deviates from the sum rule that its integral should vanish. The finite spin-orbit polarization between the two main photoemission peaks appears to be related to the nonvanishing magnetic (circular as well as linear) dichroism in this region. The influence of photoelectron diffraction[28,49] on magnetic dichroism, for which evidence was found here, as well as on spin polarization has to be incorporated in an analysis of magnetic dichroism.

In our initial experiments on magnetic linear dichroism[21] on the Fe $3p$ level we studied also circular dichroism on the same samples under identical conditions.[42] It was noticed that the asymmetry showed the same spectral dependence in both cases;[42] there was, however, a difference in the size of the linear and circular dichroisms. The observed linear dichroism was larger than the circular one; however, taking the finite degree of circular polarization into account, the asymmetry in circular dichroism was about $\frac{3}{2}$ times that of linear dichroism. The close similarity of the dichroisms was an empirical indication suggesting that the underlying physics is the same in both cases.[42] This view has been substantiated by a number of theoretical analyses,[24,33,35,36] as well as by the analysis given here. For the Fe $2p$ level, there are to date no experimental results on circular dichroism similar to the results shown here for linearly polarized light which allow a detailed comparison. As the high quality of the present data shows, the study of magnetic dichroism using linearly polarized light is a viable alternative to the use of circular dichroism. The high flux and nearly 100% polarization provided at state-of-the-art synchrotron beamlines, combined with efficient spin analysis, allows one to achieve high energy resolution in spin-resolved studies on the $2p$ levels of the $3d$ transition metals.

ACKNOWLEDGMENTS

It is a pleasure to thank T. Möller and F. Federmann of HASYLAB for help in running the fabulous BW3 beamline. Funding by the Bundesministerium für Forschung and Technologie (BMFT) under Grant No. 05 5PF DAB 3 as well as by the Deutsche Forschungsgemeinschaft (DFG) within Project SFB 166/G7 is gratefully acknowledged. N.A.C. would like to express his gratitude to the Alexander von Humboldt-Stiftung for financial support and to Bielefeld University for the hospitality extended to him during his stay there.

*Permanent address: State Academy of Aerospace Instrumentation, 190000 St. Petersburg, Russia.

[1] C. S. Fadley, D. A. Shirley, A J. Freeman, P. S. Bagus, and J. V. Mallow, Phys. Rev. Lett. **23**, 1397 (1969); C. S. Fadley and D. A. Shirley, Phys. Rev. A **2**, 1109 (1970); J. F. van Acker, Z. M. Stadnik, J. C. Fuggle, H. J. W. M. Hoekstra, K. H. J. Buschow, and G. Stroink, Phys. Rev. B **37**, 6827 (1988).

[2] J. L. Erskine and E. A. Stern, Phys. Rev. B **12**, 5016 (1976).

[3] G. Schütz *et al.*, Phys. Rev. Lett. **58**, 737 (1987); Z. Phys. B **75**, 495 (1989).

[4] C. T. Chen, F. Sette, Y. Ma, and S. Modesti, Phys. Rev. B **42**, 7262 (1991).

[5] L. Baumgarten, C. M. Schneider, H. Petersen, F. Schäfers, and J. Kirschner, Phys. Rev. Lett. **65**, 492 (1990).

[6] B. T. Thole, P. Carra, F. Sette, and G. van der Laan, Phys. Rev. Lett. **68**, 1943 (1992).

[7] Y. Wu, J. Stöhr, B. D. Hermsmeier, M. G. Samant, and D. Weller, Phys. Rev. Lett. **69**, 2307 (1992).

[8] C. Carbone and E. Kisker, Solid State Commun. **65**, 1107 (1988).

[9] F. U. Hillebrecht, R. Jungblut, and E. Kisker, Phys. Rev. Lett. **65**, 2450 (1990).

[10] C. Carbone, R. Rochow, T. Kachel, and W. Gudat, Z. Phys. B **79**, 325 (1990); Solid State Commun. **77**, 619 (1991).

[11] T. Kachel, C. Carbone, and W. Gudat, Phys. Rev. B **47**, 15 391 (1993).

[12] B. Sinkovic, P. D. Johnson, N. B. Brookes, A. Clarke, and N. V. Smith, Phys. Rev. Lett. **65**, 1647 (1990).

[13] D. G. van Campen, R. J. Pouliot, and L. E. Klebanoff, Phys. Rev. B **48**, 17 533 (1933); L. E. Klebanoff, D. G. van Campen, and R. J. Pouliot, in *Magnetic Ultrathin Films — Multilayers and Surfaces, Interfaces and Characterization*, edited by B. T. Jonker, S. A. Chambers, R. F. C. Farrow, C. Chappert, R. Clarke, W. J. M. de Jonge, T. Egami, P. Grünberg, K. M. Krishnan, E. E. Marinero, C. Rau, and S. Tsunashima, MRS Symposia Proceedings No. 313 (Materials Research Society, Pittsburgh, 1993), p. 589.

[14] N. A. Cherepkov, Sov. Phys. JETP **38**, 463 (1974).

[15] G. Schönhense, Phys. Rev. Lett. **44**, 640 (1980). For a review, see U. Heinzmann and G. Schönhense, in *Polarized Electrons in Surface Physics*, edited by R. Feder (World Scientific, Singapore, 1985), p. 467 ff.

[16] Ch. Roth, F. U. Hillebrecht, H. B. Rose, and E. Kisker, Phys. Rev. Lett. **73**, 1943 (1994).

[17] H. B. Rose, F. U. Hillebrecht, Ch. Roth, and E. Kisker, Phys. Rev. B **53**, 1630 (1996).

[18] C. M. Schneider, D. Venus, and J. Kirschner, Phys. Rev. B **45**, 5041 (1992).

[19] D. P. Pappas, G. D. Waddill, and J. G. Tobin, J. Appl. Phys. **73**, 5936 (1993); G. D. Waddill, J. G. Tobin, and D. P. Pappas, Phys. Rev. B **46**, 552 (1992).

[20] G. van der Laan, M. A. Hoyland, M. Surman, C. F. J. Flipse, and B. T. Thole, Phys. Rev. Lett. **69**, 3827 (1992).

[21] Ch. Roth, F. U. Hillebrecht, H. B. Rose, and E. Kisker, Phys. Rev. Lett. **70**, 3479 (1993).

[22] G. Rossi, F. Sirotti, N. A. Cherepkov, F. Combet-Farnoux, and G. Panaccione, Solid State Commun. **90**, 557 (1994).

[23] F. U. Hillebrecht, Ch. Roth, H. B. Rose, W.-G. Park, and E. Kisker (unpublished); F. U. Hillebrecht, H. B. Rose, Ch. Roth, and E. Kisker, J. Magn. Magn. Mater. **148**, 49 (1995).

[24] N. A. Cherepkov, Phys. Rev. B **50**, 13 813 (1994).

[25] N. A. Cherepkov and V. V. Kuznetzov, J. Phys. Condens. Matter (to be published).

[26] F. U. Hillebrecht and W.-D. Herberg, Z. Phys. B **93**, 299 (1994); A. Fanelsa, R. Schellenberg, F. U. Hillebrecht, and E. Kisker, Solid State Commun. **96**, 291 (1995).

[27] M. Getzlaff, Ch. Ostertag, G. H. Fecher, N. A. Cherepkov, and G. Schönhense, Phys. Rev. Lett. **73**, 3030 (1994).

[28] H. B. Rose, F. U. Hillebrecht, E. Kisker, R. Denecke, and L. Ley,

J. Magn. Magn. Mater. **148**, 62 (1995); H. B. Rose, Ph.D. thesis, Düsseldorf, 1996.
[29] W. Kuch, M. T. Lin, W. Steinhögl, C. M. Schneider, D. Venus, and J. Kirschner, Phys. Rev. B **51**, 609 (1995).
[30] B. T. Thole and G. van der Laan, Phys. Rev. Lett. **67**, 3306 (1991); Phys. Rev. B **44**, 12 424 (1991).
[31] S. Imada and T. Jo, J. Phys. Soc. Jpn. **60**, 2843 (1991).
[32] D. Venus, L. Baumgarten, C. M. Schneider, C. Boeglin, and J. Kirschner, J. Phys. Condens. Matter **3**, 1239 (1993).
[33] D. Venus, Phys. Rev. B **48**, 6144 (1993); **49**, 8821 (1994).
[34] B. T. Thole and G. van der Laan, Phys. Rev. B **49**, 9613 (1994).
[35] G. van der Laan and B. T. Thole, Solid State Commun. **92**, 427 (1994).
[36] B. T. Thole and G. van der Laan, Phys. Rev. **50**, 11 474 (1994).
[37] Y. Kakehashi, Phys. Rev. B **31**, 7842 (1985).
[38] H. Ebert, J. Phys. Condens. Matter **1**, 9111 (1989).
[39] H. Ebert, L. Baumgarten, C. M. Schneider, and J. Kirschner, Phys. Rev. B **44**, 4406 (1991).
[40] H. Ebert and G.-Y. Guo, J. Magn. Magn. Mater. **148**, 174 (1995).
[41] E. Tamura, G. D. Waddill, J. G. Tobin, and P. A. Sterne, Phys. Rev. Lett. **73**, 1533 (1994).
[42] F. U. Hillebrecht, Ch. Roth, H. B. Rose, M. Finazzi, and L. Braicovich, Phys. Rev. B **51**, 9333 (1995).
[43] R. Reininger and V. Saile, Nucl. Instrum. Methods Phys. Res. Sect. A **288**, 343 (1990); A. R. B. de Castro and R. Reininger, Rev. Sci. Instrum. **63**, 1317 (1992); Th. Möller, Synchrotron Radiat. News **6**, 16 (1993); C. U. S. Larsson, A. Beutler, O. Björneholm, F. Federmann, U. Hahn, A. Rieck, S. Verbin, and T. Möller, Nucl. Instrum. Methods Phys. Res. Sect. A **337**, 603 (1994).
[44] G. Waller and U. Gradmann, Phys. Rev. B **26**, 6330 (1982).
[45] U. Gradmann, G. Waller, R. Feder, and E. Tamura, J. Magn. Magn. Mater. **31–34**, 883 (1983).
[46] D. Tillmann, R. Thiel, and E. Kisker, Z. Phys. B **77**, 1 (1989).
[47] D. P. Siddons, M. Hart, Y. Amemiya, and J. B. Hastings, Phys. Rev. Lett. **64**, 1967 (1990); J. B. Kortright, M. Rice, and R. Carr, Phys. Rev. B **51**, 10 240 (1995).
[48] S. Doniach and M. Sunjic, J. Phys. C **3**, 285 (1970).
[49] F. U. Hillebrecht, H. B. Rose, T. Kinoshita, Y. U. Idzerda, G. van der Laan, R. Denecke, and L. Ley, Phys. Rev. Lett. **75**, 2883 (1995).
[50] D. P. Pappas, K.-P. Kämper, B. P. Miller, H. Hopster, D. E. Fowler, C. R. Brundle, A. C. Luntz, and Z.-X. Shen, Phys. Rev. Lett. **66**, 504 (1991).
[51] H. Hopster, R. Raue, and R. Clauberg, Phys. Rev. Lett. **53**, 695 (1984).
[52] S. F. Alvarado, R. Feder, H. Hopster, F. Ciccacci, and H. Pleyer, Z. Phys. B **49**, 129 (1982).
[53] N. A. Cherepkov and V. V. Kuznetzov, J. Phys. B **22**, L405 (1989).
[54] K. Blum, *Density Matrix Theory and Applications* (Plenum, New York, 1981).
[55] State multipoles are the characteristics of the state of a system which are introduced instead of the density matrix, i.e., the density matrix can be represented as an expansion in state multipoles. This expansion is exactly similar to the expansion of the product of two spherical functions in a series of one spherical function and $3j$ coefficients. State multipoles are tensors, and they explicitly show the character of polarization of a given state. The first-rank tensor is a vector, and therefore the state with a nonzero state multipole of the first rank is called oriented. A state with nonzero state multipole of the second rank is called aligned.
[56] N. A. Cherepkov, Adv. At. Mol. Phys. **19**, 395 (1983).
[57] J. W. Cooper, Phys. Rev. **128**, 681 (1962).
[58] S. M. Goldberg, C. S. Fadley, and S. Kono, J. Electron. Spectrosc. Relat. Phenom. **21**, 285 (1981).
[59] R. Nyholm, N. Martensson, A. Lebugle, and U. Axelsson (unpublished); also N. Martensson, Ph.D. thesis, Uppsala University, Uppsala, 1980.
[60] J. C. Fuggle and S. F. Alvarado, Phys. Rev. A **22**, 1615 (1980).